

# モード変換を考慮したマイクロ波探傷法の 曲がり部を持つ配管への一般適用性評価

Evaluation of general applicability of microwave NDT to pipes with a bend  
focusing on mode conversion

東北大学大学院	陳 冠任	Guanren CHEN	Non-Member
東北大学大学院	片桐 拓也	Takuya KATAGIRI	Non-Member
東北大学大学院	遊佐 訓孝	Noritaka YUSA	Member
東北大学大学院	橋爪 秀利	Hidetoshi HASHIZUME	Member

## Abstract

This study evaluates the key factors impacting on multi-mode conversion of microwave when applying microwave NDT to bent pipe inspection. Mathematical derivation demonstrates the dependence of multi-mode conversion due to a bend on three factors: the ratio of bending radius to pipe's diameter, the bend angle and the frequency normalized with the cut-off frequency of an arbitrary mode. To verify the deducting results, numerical simulations were conducted to evaluate multi-mode conversion of bent pipe adopting TE<sub>01</sub> microwave mode as excitation. Simulation results showed that in spite of different inner diameters, transmission characteristics of microwaves propagating in bent pipes manifest excellent consistency if the pipes are characterized by the same three aforementioned factors.

**Keywords:** Microwave NDT, mode conversion, bend, pipe

## 1. Introduction

Metallic pipes are widely utilized in many industrial facilities, where failures of pipes [1] may cause immense economic losses, severe environmental pollutions and even personnel casualties. Therefore, developing efficient non-destructive pipe inspecting methods becomes increasingly essential and imperative.

Microwave NDT [2] has been proposed as an advanced technology which can implement high-speed and long-range pipe inspection. Microwaves are excited at one end of the pipe and propagate inside it with very low attenuation. A reflection will occur if a flaw is situated on the inner surface of the pipe, and the location of the flaw, relative to the excitation probe, can be determined by analyzing the TOF (time of flight) of reflection signal caused by the flaw.

The applicability of microwave NDT to bent pipe inspection

has been verified experimentally in a former study [3]. Reflection signals from circumferential pipe wall thinning located behind a bend are discernable for detection, whereas they are not as clear as the results obtained using straight pipes. It is because the mode conversion of microwave at bends causes the presence of several modes, which gives rise to multiple peaks and obscure reflection in time domain. Factors affecting mode conversion due to bend were investigated preliminarily [4]. The results showed that mode conversion due to a bend was determined by three factors: the ratio of pipe's bending radius to diameter, the normalized frequency and the bend angle. However, mathematical derivation in the former study only demonstrated the dependence of single-mode conversion, while multi-mode conversion usually occurs with the width of sweeping frequency span increasing. Moreover, in the numerical simulation of the former study, only TM<sub>01</sub> mode was used as excitation, and only one scenario of simulation condition was discussed.

In order to evaluate the general applicability of microwave NDT to bent pipe inspection, the generality of the dependence of multi-mode conversion due to a bend should be studied deeply

---

連絡先: 陳冠任 〒980-8579 仙台市青葉区荒巻字青葉  
6-6-01-2、東北大学大学院工学研究科 量子エネルギー  
工学専攻  
E-mail: chen.guanren.q8@dc.tohoku.ac.jp

and comprehensively. In this study, the dependence of multi-mode conversion due to one bend on aforementioned three factors was demonstrated theoretically. Corresponding numerical simulations for different scenarios were conducted with TE<sub>01</sub> microwave mode employed as excitation.

## 2. Mathematical derivation

Fig. 1 illustrates the mode conversion at a bend.  $r$ ,  $D$  and  $\alpha$  denote bending radius, pipe's diameter and bend angle.  $z$  is the length of the curve along which microwaves propagate. Mode conversion of microwave occurs at the bend region.

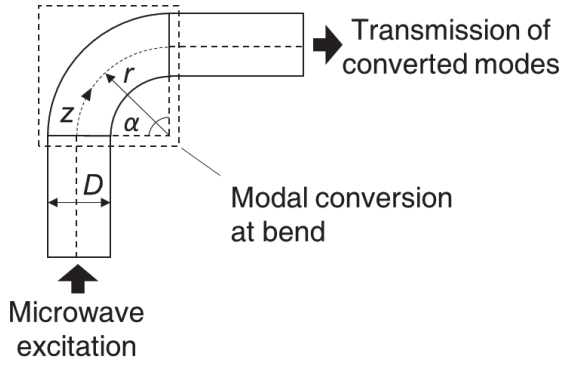


Fig. 1. Illustration of mode conversion at a bend

According to the previous study on mode conversion due to bend [5], mathematical expressions of multi-mode coupling can be interpreted in (1).

$$\begin{cases} \frac{dA_{m'n'}^+}{dz} = -j\beta_{m'n'}A_{m'n'}^+ - j\sum_{mn} C_{(m'n')(mn)}^{\pm} A_{mn}^{\pm} \\ \frac{dA_{m'n'}^-}{dz} = j\beta_{m'n'}A_{m'n'}^- + j\sum_{mn} C_{(m'n')(mn)}^{\pm} A_{mn}^{\mp} \end{cases} \quad (1)$$

where  $A$ ,  $C$  and  $\beta$  denote the amplitude of the converted mode, coupling coefficient and phase constant, respectively.  $m$ ,  $n$ ,  $m'$  and  $n'$  are mode numbers, and  $|m - m'| = 1$ . '+' and '-' refer to the forward direction and backward direction of propagation.

Since it is obvious to see that  $dz = r \cdot d\alpha$ , from Fig. 1, (1) can be rewritten as:

$$\begin{cases} \frac{dA_{m'n'}^+}{d\alpha} = -jr\beta_{m'n'}A_{m'n'}^+ - j\sum_{mn} rC_{(m'n')(mn)}^{\pm} A_{mn}^{\pm} \\ \frac{dA_{m'n'}^-}{d\alpha} = jr\beta_{m'n'}A_{m'n'}^- + j\sum_{mn} rC_{(m'n')(mn)}^{\pm} A_{mn}^{\mp} \end{cases} \quad (2)$$

According to the definition of phase constant and the

proportional relationship between wavenumber  $k$  and frequency  $f$ ,  $r\beta_{m'n'}$  is calculated as follow:

$$\begin{aligned} r\beta_{m'n'} &= r \sqrt{k^2 - \frac{X_{m'n'}^2}{(\frac{D}{2})^2}} = \frac{2u_{01}r}{D} \sqrt{\frac{k^2}{k_{cM01}^2} - \frac{X_{m'n'}^2}{u_{01}^2}} \\ &= \frac{2u_{01}r}{D} \sqrt{\frac{f^2}{f_{cM01}^2} - \frac{X_{m'n'}^2}{u_{01}^2}} = f_0 \left( \frac{f}{f_{cM01}}, \frac{r}{D} \right) \end{aligned} \quad (3)$$

where  $X_{m'n'}$  is the  $n$ th zero of  $J_m(X)$  (for TM modes) or  $J_m'(X)$  (for TE modes),  $J_m(X)$  is  $m$ -rank Bessel function.  $k_{cM01}$  and  $f_{cM01}$  denote the cut-off wavenumber and the cut-off frequency of TM<sub>01</sub> mode, and  $u_{01}$  is given by  $u_{01} = 2k_{cM01}/D$ . From (4), it is evident that  $r\beta_{m'n'}$  is dependent on  $r/D$  as well as  $ff_{cM01}$ . Virtually,  $f$  can be normalized with the cut-off frequency of any mode.

Besides, taking the coupling coefficient from TE to TM mode as an instance,  $rC_{(m'n')(mn)}^{\pm}$  can be expressed as follows:

$$\begin{aligned} rC_{(m'n')(mn)}^{\pm} &= \frac{-mu_{01}}{2(u_{m'n'}^2 - v_{mn}^2)\sqrt{v_{mn}^2 - m^2}} \cdot \frac{f}{f_{cM01}} \\ &\cdot \frac{\sqrt{\frac{f^2}{f_{cM01}^2} - \frac{v_{mn}^2}{u_{01}^2}} \pm \sqrt{\frac{f^2}{f_{cM01}^2} - \frac{u_{m'n'}^2}{u_{01}^2}}}{\sqrt{\sqrt{\frac{f^2}{f_{cM01}^2} - \frac{v_{mn}^2}{u_{01}^2}} \cdot \sqrt{\frac{f^2}{f_{cM01}^2} - \frac{u_{m'n'}^2}{u_{01}^2}}} \quad (4), \\ &= f_1 \left( \frac{f}{f_{cM01}} \right) \end{aligned}$$

where  $u_{mn}$  and  $v_{m'n'}$  are constants determining the cut-off frequencies of TM<sub>mn</sub> and TE<sub>m'n'</sub> modes. The result indicates that  $rC_{(m'n')(mn)}^{\pm}$  only hinges on  $ff_{cM01}$ . Similarly, by substituting other coupling coefficients (TM to TE, TM to TM, TE to TE) into  $rC_{(m'n')(mn)}^{\pm}$ , the same consequences are able to be acquired accordingly.

Based on the above deductions, it can be easily concluded that the coefficients of (2) depend on  $r/D$  and  $ff_{cM01}$ , while the solution to (2) is a function of  $\alpha$ . Technically, how modes are converted at a bend can be determined if  $r/D$ ,  $ff_{cM01}$  and  $\alpha$  are designated.

## 3. Numerical simulation

### 3.1 Simulation model and parameters

Three-dimensional finite element simulations were performed using commercial COMSOL Multiphysics v5.0 with its RF

module. The governing equation of the simulation is:

$$\nabla \times \mu_r^{-1} (\nabla \times \mathbf{E}) - k_0^2 [\varepsilon_r - j\sigma / (\omega\varepsilon_0)] \mathbf{E} = \mathbf{0} \quad (5),$$

where  $k_0 = \sqrt{\varepsilon_0\mu_0}$  is the propagation constant in a vacuum,  $\varepsilon_0$  and  $\mu_0$  are permittivity and permeability in a vacuum,  $\omega$  is the angular velocity.  $\mathbf{E}$  denotes the vector of electric field intensity, whilst  $\sigma$  is the electrical conductivity.  $\varepsilon_r$  and  $\mu_r$  are relative permittivity and relative permeability.

The geometric model of simulation is illustrated in Fig. 2. TE<sub>01</sub> microwave mode was excited at one end of the pipe (I), while transmission characteristics of converted modes as well as TE<sub>01</sub> mode were evaluated at the other end (II). An additional PML (perfectly matched layer) was deployed at the end II to eliminate the reflections at the surface. Second-order tetrahedral were used for discretization. The simulation parameters are listed in Table 1.

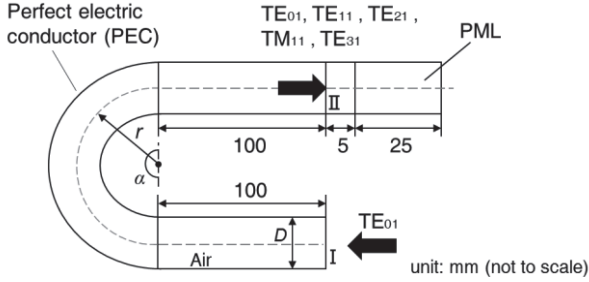


Fig. 2. Geometric model of numerical simulation

Table 1 Simulation parameters

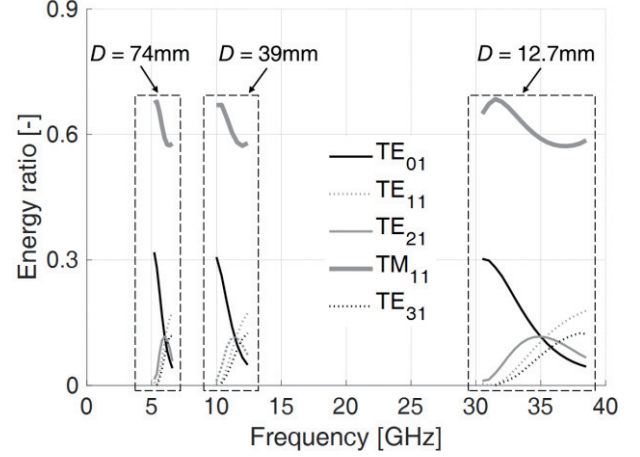
Parameter (unit)	value
$D$ (mm)	12.7, 57.5, 74
$r/D$ (-)	1, 2, 3, 4, 5
$\alpha$ (°)	90, 180
$f$ (GHz)	30.5- 38.5 ( $D = 12.7$ mm) 10 – 12.4 ( $D = 39$ mm) 5.2 - 6.6 ( $D = 74$ mm)
$ff_{cM01}$ (-)	1.68 - 2.12 (approx.)
$ff_{cE01}$ (-) *	1.05 - 1.33 (approx.)

(\*:  $f_{cE01}$  is the cut-off frequency of TE<sub>01</sub> mode)

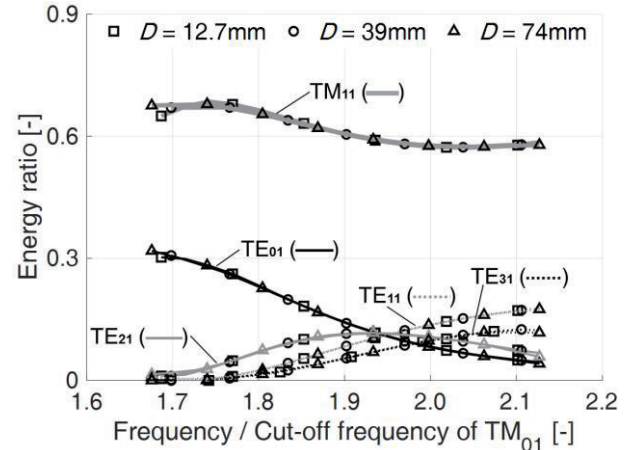
### 3.2 Simulation results

Simulation results of two scenarios ( $\alpha = 180^\circ$ ,  $r/D = 1$  and  $\alpha = 90^\circ$ ,  $r/D = 3$ ) are displayed in Fig. 3 and Fig. 4. In both two scenarios, when microwaves propagate through three bent pipes of different  $D$ , the transmission characteristics are different if  $f$  were not normalized with  $f_{cM01}$  or  $f_{cE01}$ . After normalization, the

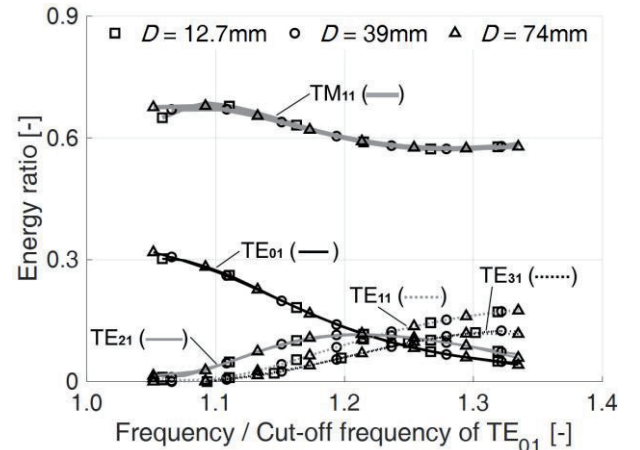
transmission characteristics of bent pipes with the same  $r/D$ , the same  $\alpha$  and the same range of  $ff_{cM01}$  reveal good consistency, despite different  $D$  (Some modes were not plotted in Fig. 4 because their values are too small). Also, from (b) and (c) in Fig. 3 and 4, it is easy to see that the cut-off frequency used for normalization can be arbitrary and has no influence on results.



(a) Without normalization

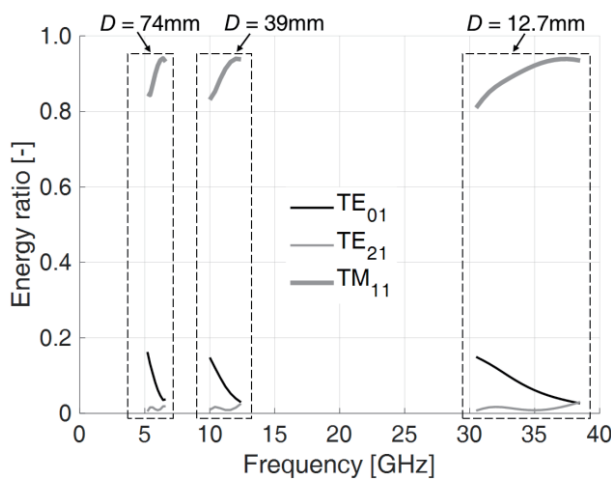


(b) With normalization ( $f$  normalized with  $f_{cM01}$ )

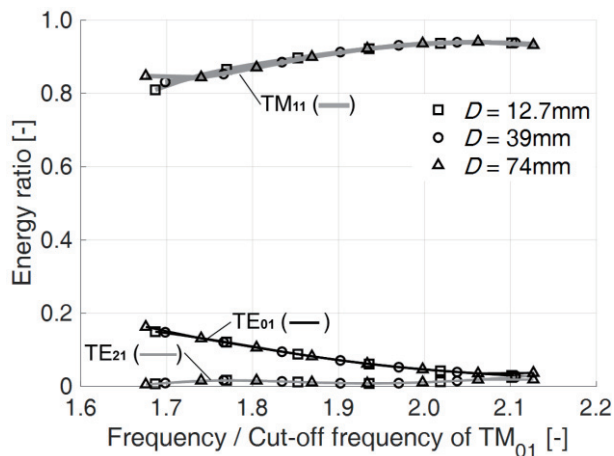


(c) With normalization ( $f$  normalized with  $f_{cE01}$ )

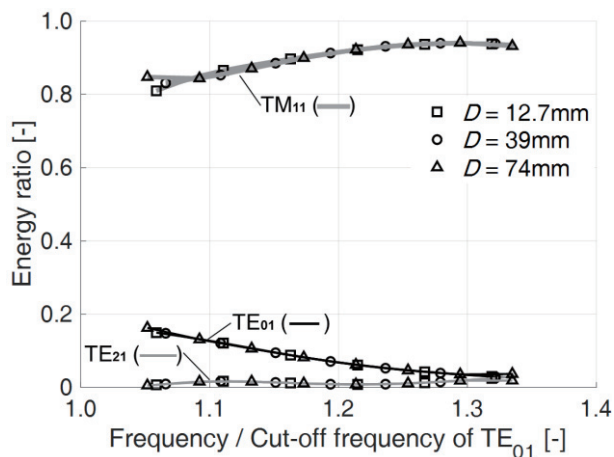
Fig. 3. Transmission characteristics ( $\alpha = 180^\circ$ ,  $r/D = 1$ )



(a) Without normalization



(b) With normalization ( $f$  normalized with  $f_{cM01}$ )



(c) With normalization ( $f$  normalized with  $f_{cE01}$ )

Fig. 4. Transmission characteristics ( $\alpha = 90^\circ$ ,  $r/D = 3$ )

multi-mode conversion due to a bend on the ratio of bending radius to diameter, the normalized frequency and the bend angle. The results of numerical simulations using  $TE_{01}$  mode as excitation comply with those of mathematical derivation, and the generality with respect to the dependence of multi-mode conversion due to bend has been verified.

## References

- [1] <http://www.sozogaku.com/fkd/en/>
- [2] K. Sugawara et al., "Development of NDT method using electromagnetic waves", JSAEM Stud. Appl. Electromagn. Mech., Vol. 10, 2001, pp. 313-316.
- [3] S. Uoshita et al., "Long-range inspection of a pipe with a bend using microwaves", the 18th international symposium on applied electromagnetics and mechanics, Chamonix-Mont-Blanc, France, September 2017, pp. 3-6.
- [4] 陳冠任ら, "マイクロ波探傷による配管検査を考慮した曲がり部におけるモード変換の影響因子の評価", 日本非破壊検査協会東北支部第6回支部会・講演会, 仙台, 2018, pp. 3
- [5] H. Li and M. Thumm, "Mode conversion due to curvature in corrugated waveguides", International Journal of Electronics, Vol. 71, No. 2, 1991, pp. 333-347.

## 4. Conclusion

This study theoretically demonstrated the dependence of